Bioorganic & Medicinal Chemistry Letters 20 (2010) 6483–6488

Contents lists available at ScienceDirect

Bioorganic & Medicinal Chemistry Letters

journal homepage: www.elsevier.com/locate/bmcl

Discovery of cell-active phenyl-imidazole Pin1 inhibitors by structure-guided fragment evolution

Andrew Potter, Victoria Oldfield [†], Claire Nunns, Christophe Fromont [‡], Stuart Ray, Christopher J. Northfield, Christopher J. Bryant, Simon F. Scrace, David Robinson [§], Natalia Matossova, Lisa Baker, Pawel Dokurno, Allan E. Surgenor, Ben Davis, Christine M. Richardson [¶], James B. Murray, Jonathan D. Moore *

Vernalis (R&D) Ltd, Granta Park, Great Abington, Cambridge CB21 6GB, United Kingdom

ARTICLE INFO

Article history:
Received 28 July 2010
Revised 6 September 2010
Accepted 10 September 2010
Available online 17 September 2010

Keywords:
Pin1
Peptidyl prolyl isomerase
Fragments
Cancer

ABSTRACT

Pin1 is an emerging oncology target strongly implicated in Ras and ErbB2-mediated tumourigenesis. Pin1 isomerizes bonds linking phospho-serine/threonine moieties to proline enabling it to play a key role in proline-directed kinase signalling. Here we report a novel series of Pin1 inhibitors based on a phenyl imidazole acid core that contains sub-μM inhibitors. Compounds have been identified that block prostate cancer cell growth under conditions where Pin1 is essential.

The parvulin-type rotamase, Pin1, catalyzes *cis*/*trans* isomerisation around the peptidyl bond linking phospho-serine/threonine and proline residues.[1] Pin1 therefore regulates the rate of certain conformational changes induced by phosphorylation/dephosphorylation of its substrates. As proline-directed protein kinases and phosphatases only recognize Ser/Thr-Pro moieties in the *trans* conformation as substrates,[2–4] Pin1 also regulates signalling dynamics for pathways involving cyclin-dependent kinases, MAP kinases and GSK3.[5] Pin1 is frequently overexpressed in tumours[6] and in prostate cancer, overexpression is also associated with poor prognosis.[7] Pin1-deficient mice are viable and their cells resistant to transformation by Ras and ErbB2.[8,9] Consequently, there are grounds to anticipate Pin1 inhibitors will be useful for cancer therapy.

The irreversible Pin1 inhibitor, juglone (**1**), has been used extensively in studies addressing the role of Pin1 inside cells and the therapeutic potential of Pin1 inhibition in vivo.[10–13] Juglone, however, lacks selectivity[12] and is not a suitable start point for drug discovery. Steady progress has been made in the identification of peptidic Pin1 inhibitors,[14–16] culminating in cyclic peptides capable of blocking Pin1 activity inside cells in the sub-μM range.[17] In addition, several cell-active small molecules have been claimed to act via Pin1 inhibition including several cinnamic acid derivatives[18] and a series of aryl indanyl ketones that reduce β-catenin levels and suppress p53-dependent transcription as would be expected for a Pin1 inhibitor.[19] Unfortunately, crystallographic information defining the binding mode of these small molecules has not emerged.

Drug discovery against Pin1 has been reported to be challenging: the major problem is finding verified hits as start points. Pfizer have disclosed that they screened 10^6 compounds versus Pin1 without finding any hits whose binding to target can be verified by NMR or isothermal calorimetry.[20] Taking an alternative approach to hit identification has proved fruitful: Pfizer designed a series of phosphate-containing aminophenyl-propanols[20] that were subsequently evolved into a series of phenylalanines that inhibited Pin1, a property shared with their styryl analogues.[21] Vernalis have disclosed a number of benzimidazole- and napthylalanine based inhibitors of Pin1 that were evolved from an indole carboxylate fragment (**2**) identified in an NMR-based screen.[22] Indole and benzimidazole alanines have also been identified as Pin1 inhibitors by Pfizer.[23]

Several members of our benzimidazole series of Pin1 inhibitors had impressive activity (~100 nM) versus the target in vitro, but failed to suppress Pin1 activity in cells due to poor permeability. Activity versus cells could be obtained by reducing the polar surface area of the molecules by replacing the benzimidazole moiety with a naphthyl group, but this led to a 10–20-fold loss

* Corresponding author.
E-mail address: j.moore@vernalis.com (J.D. Moore).
† Present address: Haddow Laboratories, Institute of Cancer Research, 15 Cotswold Rd, Belmont, Sutton, Surrey SM2 5NG, UK.
‡ Present address: School of Pharmacy, University Park, Nottingham, NG7 2RD, UK.
§ Present address: Division of Biological Chemistry & Drug Discovery, College of Life Sciences, James Black Centre, University of Dundee, Dundee, DD1 5EH, UK.
¶ Present address: Biofocus DPI, Chesterford Research Park, Saffron Walden, Essex, CB10 1XL, UK.

0960-894X/$ - see front matter © 2010 Elsevier Ltd. All rights reserved.
doi:10.1016/j.bmcl.2010.09.063

in potency.[22] For a variety of reasons, the benzimidazole/naphthyl series were not progressed further and we sought new fragment hits that might be more suitable for evolution into drugs.

Nine hundred fragments[24] were tested for their ability to inhibit Pin1-mediated isomerisation of the peptide AApSPR-pNA in a protease coupled assay[25,26] at a compound concentration of 2 mM. Forty putative 'hits' were identified, including the indole carboxylate and benzimidazole propionic acids reported previously.[22] Two-dimensional NMR experiments, however, only verified binding for 2 of the 37 novel 'hits' to Pin1 (see Fig. S1 for an example). In the absence of corroborative data we cannot exclude the possibility that a given compound inhibits Pin1-mediated peptide isomerisation via non-specific mechanisms such as forming colloidal aggregates.[27]

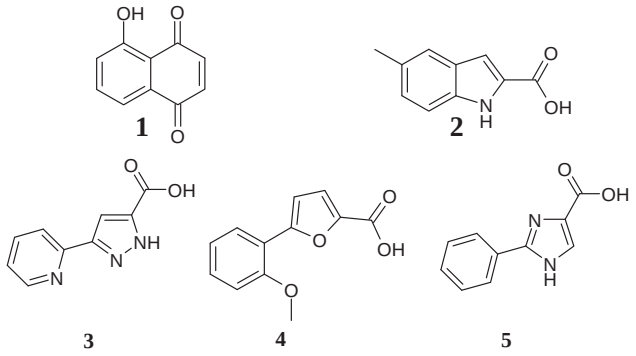

From soaking experiments with crystals of Pin1R14A protein[28] we obtained a bound structure for one the NMR-verified compounds, the pyridine-pyrazole acid **3** (Pin1 IC_{50} 720 μM) (Fig. 1a). There are notable similarities between the binding mode of **3** and the indole carboxylate fragment (**2**) identified previously (see Fig. S2):[22,26] the Lys63-interacting carboxylate moieties are identically positioned and one of the pyrazole nitrogens of **3** overlaps with the indole NH of **2** and recapitulates the hydrogen-bond interaction with Cys113. A variety of near neighbours of **3** were acquired and assayed for their ability to inhibit Pin1 and soak into Pin1 crystals. Crystal structure were obtained for several analogues bound to Pin1, including the phenyl furan acid **4** (Pin1 IC_{50} >1000 μM), in which the heteroatom of the five-membered ring of the ligand interacts via a hydrogen bond with Ser154, which is on the opposite site of the Pin1 active site from Cys113 (Fig. 1b). The starting point for our medicinal chemistry, however, was the most potent of the near neighbours identified: the phenyl-imidazole acid, **5** (IC_{50} 180 μM; ligand efficiency (LE) 0.34), which makes H-bond interactions with both Cys113 and Ser154 via its imidazole nitrogens (Fig. 1c).

We began by exploiting a literature route[29] to synthesise analogues of **5** bearing a methyl moiety at the 5-position of the imidazole ring, and investigated SAR around the pendant phenyl ring (Scheme 1). The commercially available ylide (**6**) was condensed with acetyl chloride and the resulting phosphanylidene (**7**), oxidised to tricarbonyl (**8**) by Oxone™. The desired imidazoles were then prepared by refluxing the tricarbonyl (**8**) and corresponding aldehyde with ammonium acetate under acidic conditions. Typical yields of imidazoles were 60–80%. The ester of (**9**) was then saponified under basic conditions generating acids (**10**) in good overall yield.

Introduction of the methyl group at the 5-position (**10a**) of parent fragment **5**, led to a small drop in ligand efficiency (LE 0.30) (see Table 1). Structural data (Fig. S3a) suggested that elaboration of the phenyl group was only possible at the 3-position, which afforded a vector into a small hydrophobic pocket bounded by the side chains of Met130, Gln131 and Phe134. We were delighted to see a

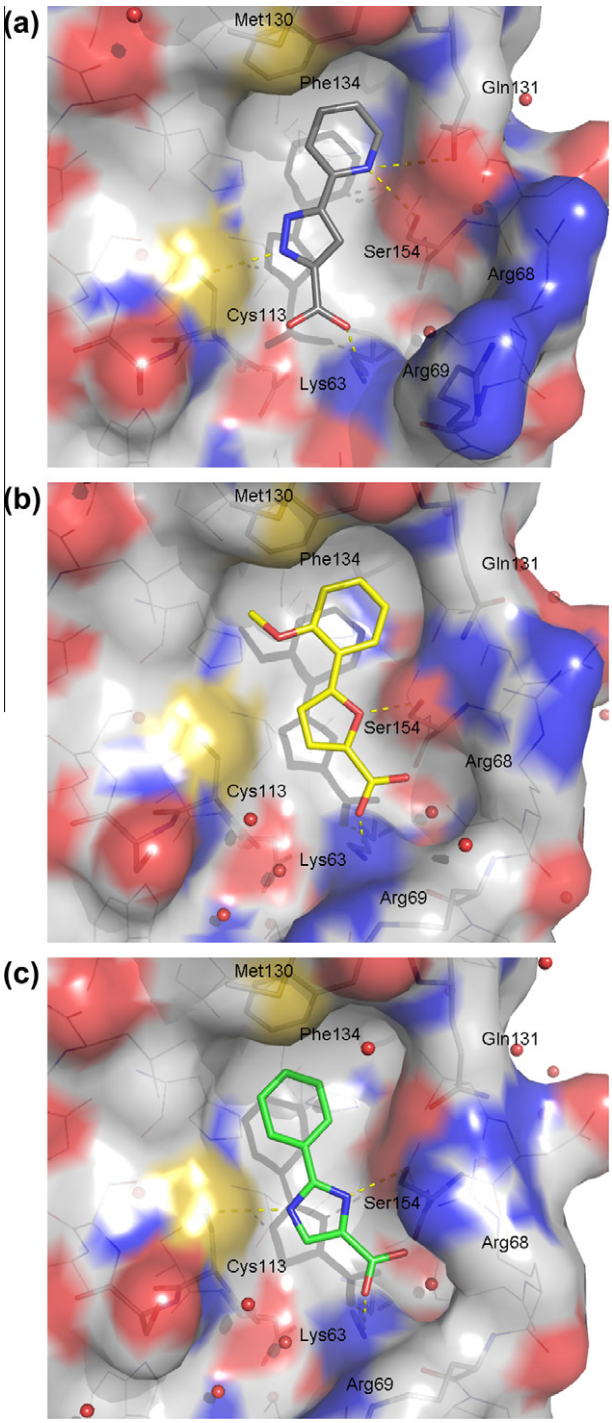

Figure 1. Pin1R14A bound crystal structures of (**a**) **3** (gray: PDB ID: 3ODK) (**b**) **4** (yellow: PDB ID 2XP3) and (**c**) **5** (green: PDB ID: 2XP4). Direct H-bonds between ligand and Pin1 are shown as yellow dashed lines, water molecules are shown in red. All three ligands occupy the catalytic site of Pin1 and make an H-bond interaction between one of the ligand's carboxylate oxygens and Lys63. The pyridine nitrogen of **3** also interact via H-bonds with both Ser154 and Gln131, while a pyrazole nitrogen makes a hydrogen bond with Cys113. The furan oxygen of **4** accepts an H-bond from Ser154. Both the imidazole nitrogens of **5** are involved in H-bond interactions: one with Cys113 and the other with Ser154.

>10-fold potency improvement by introduction of a trifluoromethyl (**10b**), methyl (**10c**), nitrile (**10d**) or chloro (**10e**) at the 3-position of the phenyl ring, which increased LE to 0.38 for the chloro substituted compound. LLE_{AT}, a normalised measure of ligand-lipophilicity efficiency (Paul Mortenson, personal communication)[26,30]

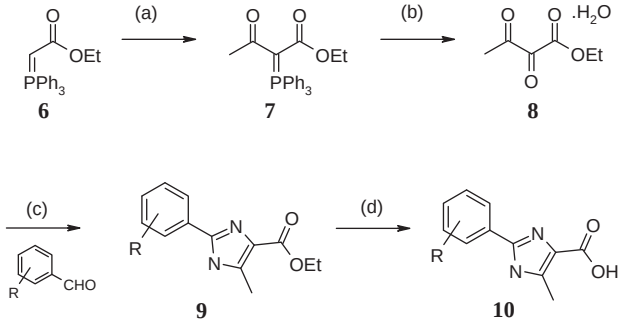

Scheme 1. Reagents and conditions: (a) AcCl, DIPEA, DCM, rt, 1 h, 98%; (b) oxoneTHF/H_2O (2:1), rt, 18 h, 100%; (c) RCHO, NH_4OAc, AcOH, 100 °C, 60–80%; (d) NaOH, EtOH, reflux, 100%.

Table 1
Biological data for 3-substituted phenyl imidazole acid Pin1 inhibitors

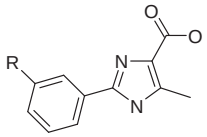

	R	Pin1 IC_{50}[a] (μM)	LE (kcal/mol/heavy atom)	LLE_{AT}[b] (kcal/mol/heavy atom)
10a	H	360	0.30	0.24
10b	CF_3	23	0.31	0.20
10c	CH_3	34	0.36	0.29
10d	CN	19	0.36	0.34
10e	Cl	20	0.38	0.27
10f	OCH_3	270	0.27	0.23

[a] IC_{50} values are means of ⩾2 determinations rounded to two significant figures. The coefficient of variance of this assay was 26% (repeat assays with compound **3** from reference 17 yielded mean IC_{50} values of 0.313 μM with standard deviation 0.081 μM; $n = 4$).

[b] LLE_{AT} is a measure of ligand-lipophilicity efficiency used at Astex Therapeutics (Paul Mortenson, personal communication) that takes into account molecule size and is ideal for tracking evolution of fragments to leads (see Supplementary data)[26]

approached or exceeded the minimum target value of 0.3 for the chloro and nitrile substituted compounds, **10d** and **10e.** The crystal structure of **10e** bound to Pin1 (Fig. S3) confirmed that the 5-position substituents occupied the hydrophobic pocket as predicted, with the position of the phenyl and imidazole rings being unaltered from the parent **10a**.[26] Larger substituents, (e.g. compound **10f**) were not beneficial nor were alternative substitutions around the phenyl ring.[31]

We considered that the vector towards the channel in Pin1 leading to Trp73 supplied by the 5-methyl on the imidazole ring provided the best opportunity to improve potency (see Fig. S3). Accessing this channel via amido acids that might make productive interactions with Arg69 was an attractive option, as the route to such compounds had already been described in the literature (Scheme 2).[32] The aldehyde (**11**) was condensed with diamino-malonitrile in DMSO and concentrated sulphuric acid. The Schiff's base produced (**12**) was then cyclised with nicotinamide and *N*-chlorosuccinamide in DMF; the dicyanoimidazole (**13**) formed in 50–60% yield. Hydrolysis of (**13**) under acidic conditions led to the diacid (**14**).

The diacids **14a** and **14b** were particularly potent and ligand-efficient inhibitors of Pin1 (Table 2). The crystal structure obtained for **14a** bound to Pin1 suggested the molecule conserved the binding mode of the other phenyl-imidazoles (Fig. S4).[26] Isothermal calorimetry confirmed these compounds bound tightly to Pin1 with 1:1 stoichiometry (ITC-derived K_d values: 1.7 μM for **14a**

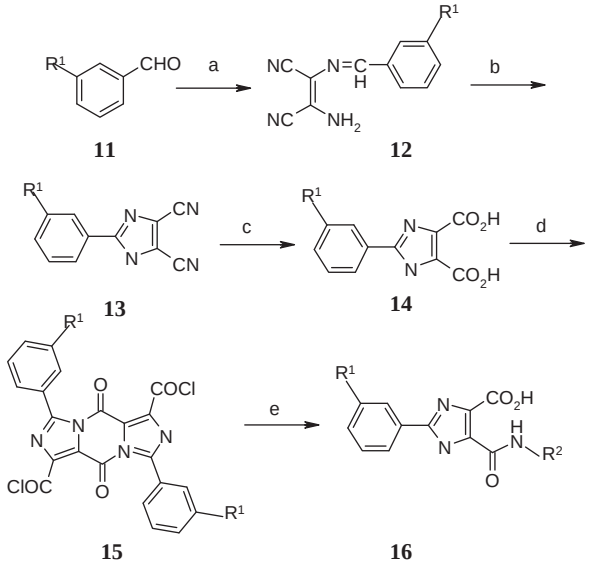

Scheme 2. Reagents and conditions: (a) diamino-malonitrile, H_2SO_4, 98%; (b) nicotinamide, *N*-chlorosuccinamide, DMF, 50–60%; (c) H_2SO_4, H_2O, reflux 70–80%; (d) $SOCl_2$, DMF, PhMe, quant; (e) R^2NH_2, NEt_3, DCM, 30–40%.

and 0.52 μM for **14b**). Diacids were chlorinated using thionylchloride to dimer (**15**). Careful treatment of this acyl chloride at low temperature with a variety of amines followed by preparative chromatography led to the amido acids (**16**), in moderate (30–40%) yield.

Initial results in this series were not encouraging: the methyl amide (**16a**) maintained the high LE of **10a**, but LE declined for the larger secondary amides (**16b**) and (**16c**) (see Table 2). Impressive gains in affinity were obtained however, for the morpholino tertiary amide (**16d**) for which we were able to obtain a crystal structure (Fig. 2a). To our surprise, the amide substituent was not positioned in the channel leading to Trp73; instead, the unsaturated morpholine ring stacked along the hydrophobic part of the Arg68 side chain and the acid group bound to both Lys63 and Arg 69 and was orientated towards the Trp73 channel. This prompted us to further explore tertiary amides.

The *N*-benzyl *N*-acetic acid ethyl ester analogue (**16f**: Pin1 IC_{50} 8 μM) bound to Pin1 in a similar manner to **16d** with the carboxylate oriented towards Trp73 and the benzylic moiety packing along the arginine side chains (Fig. 2b). An interesting additional interaction was, however, observed between the carbonyl oxygen of the ester substituent and the secondary amine nitrogen in Arg69 (Fig. 2b). Unfortunately, **16f** did not impair proliferation of PC3 prostate cancer cells, even under the serum-starved conditions where Pin1 expression is known to be important.[33] Previous experience suggested increasing the lipophilicity of Pin1 inhibitors could improve activity vs. cells.[22] We chose to synthesise an *N*,*N*′-dibenzyl analogue as modelling suggested the aryl groups might stack with the side chains of both Arg68 and Arg69. This hypothesised binding mode could not be verified as no crystal structure could be obtained for **16g** (or any similar compound). Encouragingly, **16g** retained the potency (Pin1 IC_{50} 4 μM) of **16f** while gaining the ability to block proliferation of PC3 cells (GI_{50} 21 μM). This gain in cell activity, however, was at the expense of a move into less drug-like chemical space as LLE_{AT} declined from 0.20 for **16f** to 0.12 for **16g**.

Replacing the *N*-benzyl moiety with more polar side chains (**16h** and **16i**) yielded compounds with improved ligand efficiency and reasonable ligand lipophilic efficiency. The *N*-methyl primary amide analogue (**16i**) was particularly notable (IC_{50} 4.1 μM; LE 0.31; LLE_{AT} 0.43) and its crystal structure (Fig. 3) indicated that

Table 2
Biological data for phenyl imidazole Pin1 inhibitors

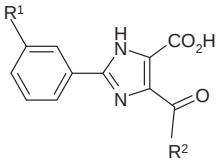

	R^1	R^2	Pin1 IC_{50}[a] (μM)	LE (kcal/mol/heavy atom)	LLE_{AT} (kcal/mol/heavy atom)	PC3 GI_{50} (μM)
14a	H	OH	1.46	0.44	0.47	ND
14b	F	OH	0.32	0.46	0.46	ND
16a	H	NHMe	80	0.29	0.34	ND
16b	H	NHEt	140	0.26	0.28	ND
16c	H	NHBn	220	0.20	0.15	ND
16d	H		15	0.28	0.34	>200
16e	H	NMeBn	31	0.23	0.18	>200
16f	H	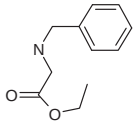	8.0	0.22	0.20	>200
16g	H	$N(Bn)_2$	4.0	0.23	0.12	21
16h	H	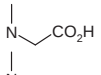	9.4	0.29	0.37	ND
16i	H	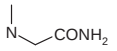	4.1	0.31	0.43	>200
16j	H	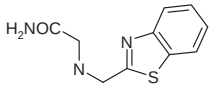	0.52	0.25	0.27	>80

[a] IC_{50} values are means of ⩾2 determinations rounded to two significant figures where appropriate. The coefficient of variance of this assay was 26%.

the ethyl amide substituent packed against the hydrophobic portion of the Arg68 side chain. Substitution of the methyl with a methyl-benzothiophene moiety resulted in **16j**, the most potent Pin1 inhibitor identified in this series (IC_{50} 0.52 μM: LE 0.25). No crystal structure of **16j** bound to Pin1 could be obtained, so it is not clear whether this molecule retains the binding mode of **16i**.

While **16i** and **16j** had encouraging potency versus Pin1 in vitro, the ability to block PC3 proliferation had been lost. We therefore reasoned that synthesising further compounds similar to **16g** might represent our best chance of progress towards identifying Pin1 inhibitors that are active in cells, even though such molecules would be highly lipophilic.

We had previously shown that 3-substitution on the phenyl ring improved potency by up to 10-fold and wondered if incorporation of a suitable group into this position of our most active tertiary amides would do likewise. We were aware, however, that consistent SAR may not be observed because the Pin1 enzyme would only be able to bind one of the slowly interconverting rotameric forms of these ligands. The rotameric forms were clearly present by NMR.[31]

In the context of **16e**, substituting a chlorine at the 3-position of the phenyl ring adjacent to the imidazole (**17**) led to a >10-fold improvement in activity vs. Pin1 (IC_{50} 2 μM) (Table 3). A crystal structure for **17** bound to Pin1R14A was obtained (Fig. 4), which indicated complete conservation of the binding mode observed for the deschloro compounds **16f** and **16i**. However, substitution of chlorine at the 3-position was not always beneficial: incorporation of the 3-substituent into the morpholino (**16d**) yielded a compound (**18**) at best equipotent versus Pin1 (IC_{50} 21 μM). 3-Chloro substitution of the phenyl in **16g** yielded a molecule (**19**) with threefold improved potency versus Pin1, albeit without a corresponding improvement in activity versus PC3 cells. The 1.4 μM IC_{50} for **19** in the trypsin-coupled functional assay was in excellent accord with ITC experiments (K_d 1.4 μM; stoichiometry 0.9). Homologation of one of the *N*-benzyl moieties to an *N*-ethylphenyl resulted in **20**, a sub-μM inhibitor of Pin1 that exhibited excellent permeability in a CaCo-2 assay (35×10^{-6}/cm)[31] and blocked the proliferation of serum-starved PC3 cells with a GI_{50} of 13 μM. **20** did not inhibit the activity of FKBP12 or cyclophilin A indicating that it specifically inhibited the PPIase activity of Pin1.

Pin1 inhibitors are anticipated to interfere with multiple cellular processes including the expression of cyclin D1,[8,34] and signalling cascades triggered by insulin.[35] We therefore asked whether **20** interfered with any of these processes as doses close to its GI_{50}. Figure 5 shows that treatment of PC3 cells with **20** phenocopies siRNA-mediated knockdown of Pin1 in reducing cyclin D1 levels in serum-starved cells (EC_{50} ~10 μM) but having no effect on cyclin E1 expression. In addition **20** impairs p70S6-Kinase phosphorylation in response to insulin (EC_{50} ~30 μM). Together these data provide considerable evidence that the effects on cells of **20** are mediated, at least in part, via inhibition of Pin1.

Fragment-based hit identification combined with structure-guided hit evolution provide a powerful means to identify novel chemical series against targets considered challenging from a drug discovery perspective. Twice using these approaches we have identified inhibitor series that contain examples exhibiting sub-μM affinity for the Pin1 target, a context where high-throughput screening has reportedly failed.[20] Though the approach used here (screening a fragment library in an enzymatic assay at a high ligand concentration) yielded a set of hits that may have been dominated by compounds interfering with Pin1-mediated peptide isomerization via non-specific mechanisms such as formation of colloidal aggregates,[27] the small number (<40) of hits and solubility of the library members enabled 2D NMR spectroscopy to pick out a novel aryl-pyrazole inhibitor that could be crystallised within Pin1. This initial hit was rapidly evolved to a series of phenyl-

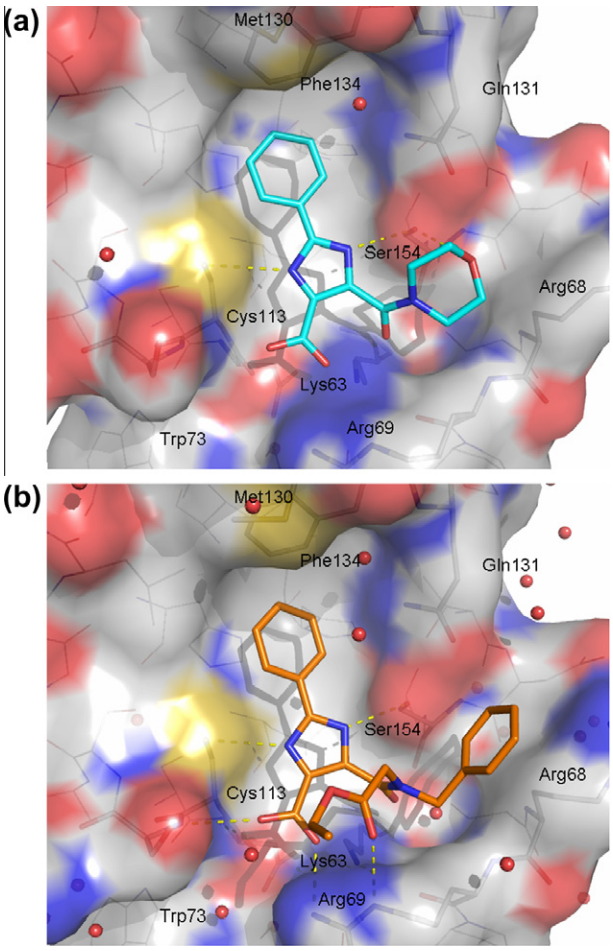

Figure 2. Crystal structures of (**a**) **16d** (cyan; PDB ID 2XP8) and (**b**) **16f** (orange; PDB ID 2XP9) in Pin1R14A. The carboxylate moiety is positioned in the channel leading towards Trp73. The morpholino group of **16d** and the benzylic moiety of **16f** stack along the hydrophobic side chain of Arg68. Water molecules are shown in red.

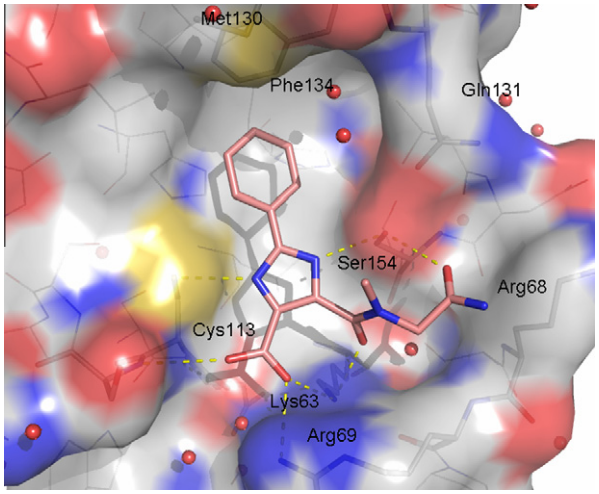

Figure 3. Crystal structure of compound **16i** in Pin1R14A (PDB ID: 2XPA). The ethyl amide of the ligand stacks along the side chain of Arg68, while the N-methyl moiety points into solvent. Waters are shown in red.

imidazoles that contained members inhibiting Pin1 with sub-μM IC_{50} values and that prevented the growth of prostate cancer cells.

The Pin1 inhibitors described in this report do not bind in the same manner as any of the classes of ligands for which binding

Table 3
Biological data for 3-chloro-phenyl-imidazole acid Pin1 inhibitors

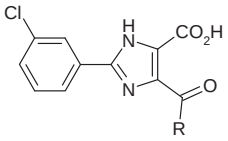

	R	Pin1 IC_{50}[a] (μM)	LE (kcal/mol/heavy atom))	LLE_{AT} (kcal/mol/heavy atom)	PC3 GI_{50} (μM)
17	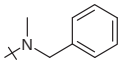	2.0	0.26	0.20	56
18	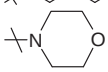	21	0.24	0.28	>200
19	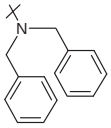	1.4	0.23	0.11	18
20	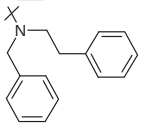	0.83	0.23	0.13	13

[a] IC_{50} values are the mean of at least two determinations and are rounded to two significant figures where appropriate. The coefficient of variance of this assay was 26%.

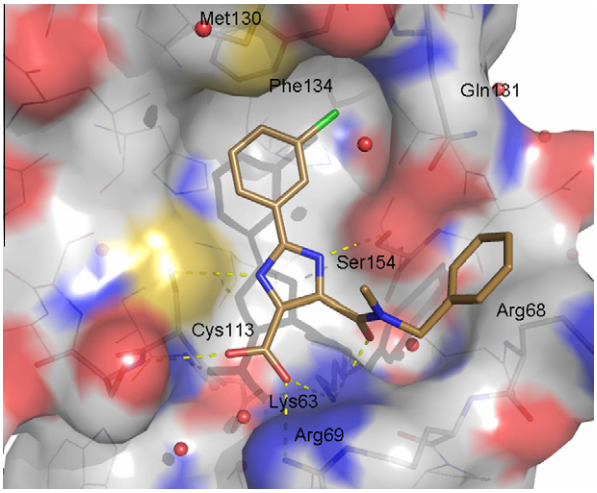

Figure 4. Crystal structure of compound **17** in Pin1R14A (PDB ID: 2XPB). Introduction of a chlorine at the 3-position of the phenyl ring did not alter the binding mode from that observed with **16f** (see Fig. 2b). Water molecules are shown in red.

modes have been reported.[20–22] Like previous series of Pin1 inhibitors, the imidazole amino acids reported here can be said to have a tripartite binding mode that comprises the following elements: a ring system occupying the hydrophobic cavity at the core of the Pin1 active site; acidic groups that interact with the basic side chains of the residues (Lys63, Arg68 and Arg69) that accommodate the phosphate in Pin1's substrates; and additional moieties that bind to hydrophobic but solvent-exposed surfaces of Pin1 adjacent to the active site. The difference is that while the previously disclosed series contact a shelf-like surface located beyond Cys113 on the other side of the binding site,[20–22] the ligands described in this report stack along the side chain of Arg68 and possibly Arg69. This novel binding mode of the imidazole amido acids raises the possibility of designing molecules that occupy novel

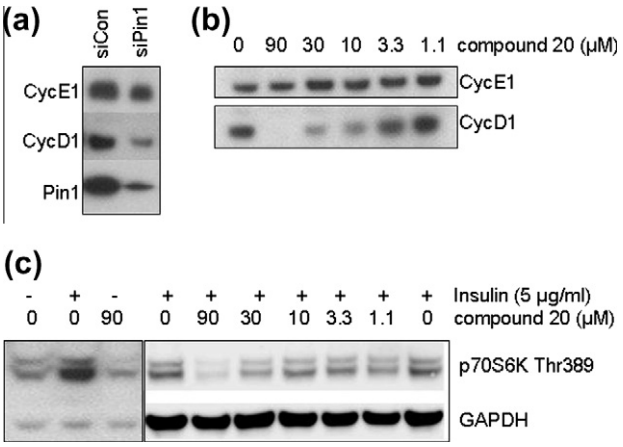

Figure 5. Compound **20** modulates biomarkers dependent upon Pin1 function. (a) Transfection of siRNA vs. Pin1 reduces expression of cyclin D1, but cyclin E1 levels are unaffected. (b) 6 h exposure to **20** reduces cyclin D1 levels, but cyclin E levels are unaffected. (c) 20 min stimulation with insulin increases phosphorylation of p70S6 kinase on Thr389; this response is blocked by 60 min pre-treatment with **20**. All data shown is from cells cultured in serum-free conditions for at least 24 h before cells were harvested.

combinations of surfaces on Pin1, providing opportunities to improve potency and/or the physiochemical properties of the compounds so that they occupy drug-like chemical space. Improvements in both regards will be necessary to identify Pin1 inhibitors suitable for use as drugs: both of our medicinal chemistry programs directed against Pin1 have failed to find compounds capable of modulating Pin1 activity in cells in the sub-μM range. The nature of the Pin1 active site makes it difficult to optimise hits into drug-like molecules: one end is dominated by three positively charged residues, the other end is a narrow yet shallow hydrophobic pocket. The ligands we have identified as Pin1 inhibitors all contain a carboxylate groups and the most potent compounds have very low permeability in Caco-2 assays.[22,31] The only way we have found to obtain activity in cells has been to add lipophilic groups, which has compromised the drug-likeness of our compounds. Despite our experiences, fragment based approaches to hit identification remain attractive route towards finding Pin1 inhibitors, because a wide region of chemical space can be sampled with a relatively small compound library. Success, however, is contingent on having suitable initial hits in the library to be screened.

Acknowledgements

The authors thank Dr. Martin Drysdale for valuable discussions, Heather Simmonite for expert assistance with compound structure determination by NMR spectroscopy and Dr. Loic Le Strat for chromatographic support.

Supplementary data

Supplementary data associated with this article can be found, in the online version, at doi:10.1016/j.bmcl.2010.09.063.

References and notes

1. Lu, K. P.; Zhou, X. Z. *Nat. Rev. Mol. Cell Biol.* **2007**, *8*, 904.
2. Weiwad, M.; Kullertz, G.; Schutkowski, M.; Fischer, G. *FEBS Lett.* **2000**, *478*, 39.
3. Brown, N. R.; Noble, M. E.; Endicott, J. A.; Johnson, L. N. *Nat. Cell Biol.* **1999**, *1*, 438.
4. Zhou, X. Z.; Kops, O.; Werner, A.; Lu, P. J.; Shen, M.; Stoller, G.; Küllertz, G.; Stark, M.; Fischer, G.; Lu, K. P. *Mol. Cell.* **2000**, *6*, 873.
5. Lu, K. P.; Finn, G.; Lee, T. H.; Nicholson, L. K. *Nat. Chem. Biol.* **2007**, *3*, 619.
6. Bao, L.; Kimzey, A.; Sauter, G.; Sowadski, J. M.; Lu, K. P.; Wang, D. G. *Am. J. Pathol.* **2004**, *164*, 1727.
7. Ayala, G.; Wang, D.; Wulf, G.; Frolov, A.; Li, R.; Sowadski, J.; Wheeler, T. M.; Lu, K. P.; Bao, L. *Cancer Res.* **2003**, *63*, 6244.
8. Liou, Y. C.; Ryo, A.; Huang, H. K.; Lu, P. J.; Bronson, R.; Fujimori, F.; Uchida, T.; Hunter, T.; Lu, K. P. *Proc. Natl. Acad. Sci. U.S.A.* **2002**, *99*, 1335.
9. Ryo, A.; Liou, Y. C.; Wulf, G.; Nakamura, M.; Lee, S. W.; Lu, K. P. *Mol. Cell. Biol.* **2002**, *22*, 5281.
10. Hennig, L.; Christner, C.; Kipping, M.; Schelbert, B.; Rücknagel, K. P.; Grabley, S.; Küllertz, G.; Fischer, G. *Biochemistry* **1998**, *37*, 5953.
11. Rippmann, J. F.; Hobbie, S.; Daiber, C.; Guilliard, B.; Bauer, M.; Birk, J.; Nar, H.; Garin-Chesa, P.; Rettig, W. J.; Schnapp, A. *Cell Growth Differ.* **2000**, *11*, 409.
12. Fila, C.; Metz, C.; van der Sluijs, P. *J. Biol. Chem.* **2008**, *283*, 21714.
13. Esnault, S.; Braun, R. K.; Shen, Z. J.; Xiang, Z.; Heninger, E.; Love, R. B.; Sandor, M.; Malter, J. S. *PLoS One* **2007**, *21*, e226.
14. Zhang, Y.; Füssel, S.; Reimer, U.; Schutkowski, M.; Fischer, G. *Biochemistry* **2002**, *41*, 11868.
15. Wildemann, D.; Erdmann, F.; Alvarez, B. H.; Stoller, G.; Zhou, X. Z.; Fanghänel, J.; Schutkowski, M.; Lu, K. P.; Fischer, G. *J. Med. Chem.* **2006**, *49*, 2147.
16. Zhao, S.; Etzkorn, F. A. *Bioorg. Med. Chem. Lett.* **2007**, *17*, 6615.
17. Liu, T.; Liu, Y.; Kao, H.-Y.; Pei, D. *J. Med. Chem.* **2010**, *53*, 2494.
18. Bayer, E.; Thutewohl, M.; Christner, C.; Tradler, T.; Osterkamp, F.; Waldmann, H.; Bayer, P. *Chem. Commun. (Camb).* **2005**, 516.
19. Daum, S.; Erdmann, F.; Fischer, G.; Féaux de Lacroix, B.; Hessamian-Alinejad, A.; Houben, S.; Frank, W.; Braun, M. *Angew. Chem., Int. Ed.* **2006**, *45*, 7454.
20. Guo, C.; Hou, X.; Dong, L.; Dagostino, E.; Greasley, S.; Ferre, R. A.; Marakovits, J.; Johnson, M. C.; Matthews, D.; Mroczkowski, B.; Parge, H.; VanArsdale, T.; Popoff, I.; Margosiak, S.; Thomson, J.; Los, G.; Murray, B. W. *Bioorg. Med. Chem. Lett.* **2009**, *19*, 5613.
21. Dong, L.; Marakovits, J.; Hou, X.; Guo, C.; Greasley, S.; Dagostino, E.; Ferre, R.-A.; Johnson, C.; Kraynov, E.; Thomson, J.; Pathak, V.; Murray, B. W. *Bioorg. Med. Chem. Lett.* **2010**, *20*, 2210.
22. Potter, A. J.; Ray, S.; Gueritz, L.; Nunns, C. L.; Bryant, C. J.; Scrace, S. F.; Matassova, N.; Baker, L.; Dokurno, P.; Robinson, D. A.; Surgenor, A. E.; Davis, B.; Murray, J. B.; Richardson, C. M.; Moore, J. D. *Bioorg. Med. Chem. Lett.* **2010**, *20*, 586.
23. Do, Q.-Q. T.; Guo, C.; Humphries, P. S.; Marakovits, J. T.; Dong, L.; Hou, X.; Johnson, M. C. PCT Int. Appl. WO2006040646, 2006.
24. Baurin, N.; Aboul-Ela, F.; Barril, X.; Davis, B.; Drysdale, M.; Dymock, B.; Finch, H.; Fromont, C.; Richardson, C.; Simmonite, H.; Hubbard, R. E. *J. Chem. Inf. Comput. Sci.* **2004**, *44*, 2157.
25. Fischer, G.; Bang, H.; Berger, E.; Schellenberger, A. *Biochim. Biophys. Acta* **1984**, *791*, 87.
26. See Supplementary data.
27. McGovern, S. L.; Helfand, B. T.; Feng, B.; Shoichet, B. K. *J. Med. Chem.* **2003**, *46*, 4265.
28. Zhang, Y.; Daum, S.; Wildemann, D.; Zhou, X. Z.; Verdecia, M. A.; Bowman, M. E.; Lücke, C.; Hunter, T.; Lu, K. P.; Fischer, G.; Noel, J. P. *ACS Chem. Biol.* **2007**, *2*, 320.
29. Brackeen, M. F.; Stafford, J. A.; Feldmana, P. L.; Karanewsky, D. S. *Tetrahedron Lett.* **1993**, *34*, 7873.
30. Leeson, P. D.; Springthorpe, B. *Nat. Rev. Drug Disc.* **2007**, *6*, 881.
31. Data not shown.
32. Moriya, O.; Minamide, H.; Urata, Y. *Synthesis (Stuttgart)* **1984**, *12*, 1057.
33. Ryo, A.; Uemura, H.; Ishiguro, H.; Saitoh, T.; Yamaguchi, A.; Perrem, K.; Kubota, Y.; Lu, K. P.; Aoki, I. *Clin. Cancer Res.* **2005**, *11*, 7523.
34. Wulf, G. M.; Ryo, A.; Wulf, G. G.; Lee, S. W.; Niu, T.; Petkova, V.; Lu, K. P. *EMBO J.* **2001**, *20*, 3459.
35. Lee, N. Y.; Choi, H. K.; Shim, J. H.; Kang, K. W.; Dong, Z.; Choi, H. S. *Carcinogenesis* **2009**, *30*, 671.